A new fast multipole boundary element method for solving 2-D Stokes flow problems based on a dual BIE formulation

Y.J. Liu*

Department of Mechanical Engineering, University of Cincinnati, P.O. Box 210072, Cincinnati, OH 45221-0072, USA

Abstract

A fast multipole boundary element method (BEM) is presented in this paper for large-scale analysis of two-dimensional (2-D) Stokes flow problems based on a dual boundary integral equation (BIE) formulation. In this dual BIE formulation, a linear combination of the conventional BIE for velocity and the hypersingular BIE for traction is employed to achieve better conditioning for the BEM systems of equations. In both the velocity and traction BIEs, the direct formulations are used, that is, the boundary variables involved are the velocity and traction directly. The fast multipole formulations for both the velocity BIE and traction BIE for 2-D Stokes flow problems are presented in this paper based on the complex variable representations of the fundamental solutions. Several numerical examples are presented to study the accuracy and efficiency of the proposed approach. The numerical results clearly demonstrate the potentials of the developed fast multipole BEM for solving large-scale 2-D Stokes flow problems.
© 2007 Elsevier Ltd. All rights reserved.

Keywords: 2-D Stokes flows; Boundary element method; Fast multipole method

1. Introduction

Stokes flow problems, which are closely related to elastostatic problems, have been formulated with boundary integral equations (BIEs) and solved by the boundary element method (BEM) for decades using either direct or indirect BIE formulations (see, e.g., Refs. [1,2]). However, the conventional BEM used to solve Stokes flow problems suffer the same drawbacks as in the elasticity case, that is, it requires $O(N^3)$ operations to solve the BEM systems of equations using direct solvers or $O(N^2)$ operations using iterative solvers, with N being the number of equations. In the mid of 1980s, Rokhlin and Greengard [3–5] pioneered the innovative fast multipole method (FMM) that can be used to accelerate the solutions of BEM equations, promising to reduce both the CPU time and memory requirement in the fast multipole accelerated BEM to $O(N)$. Some of the research on fast multipole BEM for elasticity problems can be found in Refs. [6–18], which

show great promises of the BEM for solving large-scale problems. A comprehensive review of the fast multipole BIE/BEM can be found in Ref. [19] and a tutorial in Ref. [20].

For Stokes flow problems using the fast multipole BEM, there have been several approaches reported in the literature. Greengard et al. [7] developed a fast multipole formulation for directly solving the biharmonic equations in two-dimensional (2-D) elasticity with the Stokes flow as a special case. They applied Sherman's complex variable formulation to solve the biharmonic equation and presented several interesting large-scale problems. Gómez and Power [21] studied 2-D cavity flow governed by Stokes equations using both direct and indirect BIEs and the fast multipole method. They used Taylor series expansions of the kernels in real variables directly and concluded that the indirect BIE formulation with double layer potential offers better conditioning of the systems of equations and thus faster convergence with the fast multipole method. Mammoli and Ingber [22] applied the fast multipole BEM to study Stokes flow around cylinders in a bounded 2-D domain. They also employed direct and indirect BIEs

*Tel.: +1 513 556 4607; fax: +1 513 556 3390.
E-mail address: Yijun.Liu@uc.edu

with the kernels expanded using Taylor series of the real variables. Large-scale 2-D Stokes flow models were studied as well as the dynamic simulations of systems with large numbers of particles. In the context of modeling micro-electro-mechanical systems (MEMS), Ding and Ye [23] developed a fast BEM using the precorrected-FFT accelerated technique for computing drag forces using 3-D MEMS models with slip boundary conditions. Frangi et al. [24–27] have conducted extensive research using the direct BIE formulations and the fast multipole BEM for evaluating damping forces of 3-D MEMS structures in infinite fluid domains. When structures are assumed to be rigid and with no slip boundary conditions, the velocity BIE is reduced to an integral equation of the first kind, which is not well conditioned. To facilitate faster convergence of the fast multipole BEM, Frangi et al. introduced the traction BIE, which is an integral equation of the second kind, and when coupled with the velocity BIE, can provide better conditioning for the BEM systems of equations. They have applied this mixed-velocity-traction BIE technique in modeling large-scale 3-D MEMS problems with the fast multipole BEM to accurately evaluate the damping forces under both no slip and slip boundary conditions [24–27].

The BIE formulations for Stokes flow problems suffer from several "defects", such as the eigenfunctions existing in the BIEs that can cause nonunique solutions of these BIEs [1,2]. Improved or complete indirect BIE formulations have been proposed to overcome these difficulties as well as to provide better conditioning for the systems of equations (see, e.g., Refs. [21,22]). However, in indirect BIE formulations, the boundary variables are not the physical quantities needed and additional evaluations are required to obtain the demanded physical quantities like velocities and tractions on the boundary. Developing direct BIE formulations that are free from the "defects" associated with the BIE formulations for Stokes flow problems will be most advantageous. Using a coupled velocity BIE and traction BIE approach may be a promising alternative, as have been demonstrated by the work of Frangi et al. [24–27] for 3-D exterior Stokes flow problems. However, this dual BIE approach has not been tested with the BIEs for 2-D Stokes flow problems and interior domain problems, where additional difficulties arise in the solutions of the boundary-value problems and in the BIE formulations.

Another existing issue is with the computing efficiencies of the fast multipole method for 2-D problems. In the study of the 2-D fast multipole BEM for elasticity problems, it is recognized that the approach based on expansions of the kernels in complex variables [5,7,18,20] is much more efficient than approaches based on expansions of kernels in real variables. This is because each term in a series of complex variables is an analytic function, and its real and imaginary parts are harmonic functions, which closely resemble the behavior of the fundamental solution that is harmonic in nature. Thus, faster convergence can be achieved with fewer expansion terms in the fast multipole

BEM using the complex BIE formulations [5,7,18,20]. The complex variable approach can be extended to develop a fast multipole BEM for 2-D Stokes flow problems based on the dual direct BIE formulation.

In this paper, a new fast multipole BEM approach is presented for 2-D Stokes flow problems based on a direct dual BIE formulation. First, the dual BIE formulation is presented that involves the velocity and traction as the boundary variables directly. The deficiencies of the CBIE and HBIE under several special situations are discussed and the remedy to all these difficulties using a linear combination of the CBIE and HBIE is proposed. Then, the fast multipole formulations for the CBIE and HBIE are presented, with formulations for the CBIE extracted directly from those for the 2-D elasticity case using complex variables [18], while formulations for the HBIE are derived by taking derivatives of the local expansions of the CBIE using complex variables. All the moments and related M2M, M2L and L2L translations for the HBIE turn out to be identical to those for the CBIE and thus very compact and efficient fast multipole BEM code can be developed using this dual BIE formulation. Three examples are presented and the numerical results clearly show the effectiveness, accuracy and efficiency of the fast multipole BEM based on the dual BIE formulation for analyzing large-scale 2-D Stokes flow problems. Finally, discussions are given on possible improvements of the developed fast multipole BEM using the dual BIE formulation and its extensions to other applications.

2. The dual BIE formulation

Consider the following boundary-value problem for a steady-state Stokes flow problem in domain V (Fig. 1):

$$equilibrium : -p_{,i} + \mu u_{i,jj} = 0, \quad \forall \mathbf{x} \in V, \tag{1}$$

$$mass\ conservation : u_{i,i} = 0, \quad \forall \mathbf{x} \in V, \tag{2}$$

$$boundary\ conditions : u_i = f_i, \quad \forall \mathbf{x} \in S_u \text{ and}$$
$$t_i = g_i, \quad \forall \mathbf{x} \in S_t, \tag{3}$$

where u_i is the velocity, p the pressure, μ the coefficient of viscosity of the fluid, f_i and g_i the given values of velocity u_i
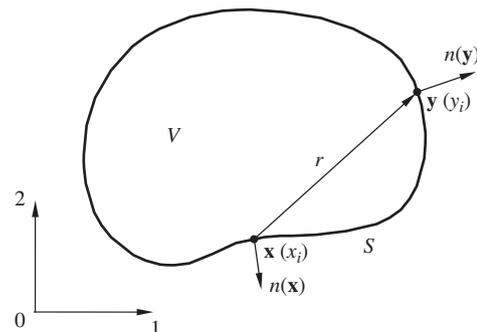

Fig. 1. Domain V and boundary S.

and traction t_i on boundary S_u and S_t ($S = S_u \cup S_t$), respectively. The stress σ_{ij} in the fluid is related to the velocity field by

$$\sigma_{ij} = -p\delta_{ij} + \mu(u_{i,j} + u_{j,i}), \quad \forall \mathbf{x} \in V \tag{4}$$

and traction on S is given by $t_i = \sigma_{ij}n_j$ with n being the outward normal of the domain (Fig. 1).

The *velocity integral representation and boundary integral* equation (CBIE) can be expressed collectively as (see, e.g., Refs. [1,2])

$$c_{ij}(\mathbf{x})u_j(\mathbf{x}) = \int_S \left[U_{ij}(\mathbf{x},\mathbf{y})t_j(\mathbf{y}) - T_{ij}(\mathbf{x},\mathbf{y})u_j(\mathbf{y}) \right] dS(\mathbf{y}),$$
$$\forall \mathbf{x} \in V \text{ or } S, \tag{5}$$

where $c_{ij} = \frac{1}{2}\delta_{ij}$ when $\mathbf{x} \in S$ that is smooth around $\mathbf{x}$, and the integral with the T kernel is a Cauchy principal-value (CPV) integral. Eq. (5) is valid for both interior and exterior problems (assuming velocity and traction fields vanish at the infinity for the latter). When $\mathbf{x} \in V$, $c_{ij} = \delta_{ij}$ and Eq. (5) is an integral representation of the velocity. The two kernel functions $U_{ij}(\mathbf{x}, \mathbf{y})$ and $T_{ij}(\mathbf{x}, \mathbf{y})$ in Eq. (5) are given by the following expressions for 2-D Stokes flow problems:

$$U_{ij}(\mathbf{x},\mathbf{y}) = \frac{1}{4\pi\mu}\left[\delta_{ij}\log\left(\frac{1}{r}\right) + r_{,i}r_{,j} - \frac{1}{2}\delta_{ij} \right], \tag{6}$$

$$T_{ij}(\mathbf{x},\mathbf{y}) = -\frac{1}{\pi r}r_{,i}r_{,j}r_{,k}n_k(\mathbf{y}), \tag{7}$$

in which $r = r(\mathbf{x}, \mathbf{y})$ is the distance between the source point $\mathbf{x}$ and field point $\mathbf{y}$ (Fig. 1), and $r_{,i} = \partial r / \partial y_i$. The constant term $-\frac{1}{2}\delta_{ij}$ in expression (6), which does not affect the BIE solution, is added for the convenience in the multipole implementation [18].

The pressure field can be represented by the following integral [1,2]:

$$p(\mathbf{x}) = \int_S [G_{,j}(\mathbf{x},\mathbf{y})t_j(\mathbf{y}) - 2\mu F_{,j}(\mathbf{x},\mathbf{y})u_j(\mathbf{y})] dS(\mathbf{y}),$$
$$\forall \mathbf{x} \in V, \tag{8}$$

in which,

$$G(\mathbf{x},\mathbf{y}) = \frac{1}{2\pi}\log\left(\frac{1}{r}\right), F(\mathbf{x},\mathbf{y}) = \frac{\partial G(\mathbf{x},\mathbf{y})}{\partial n(\mathbf{y})}$$
$$= -\frac{1}{2\pi r}r_{,k}n_k(\mathbf{y}) \tag{9}$$

are the fundamental solutions for 2-D potential problems. From Eq. (8), one can find the pressure field $p(\mathbf{x})$ in domain V once the velocity and traction fields are known on boundary S.

Taking the derivatives of Eq. (5) with $\mathbf{x} \in V$ ($c_{ij} = \delta_{ij}$) and $n_i(\mathbf{x})$ being a vector at $\mathbf{x}$, applying Eq. (4) with expressions

in (6) and (7), one has the following results:

$$\sigma_{ij}(\mathbf{x})n_j(\mathbf{x}) = -p(\mathbf{x})n_i(\mathbf{x}) + n_i(\mathbf{x})$$
$$\times \int_S \left\lfloor G_{,j}(\mathbf{x},\mathbf{y})t_j(\mathbf{y}) - 2\mu F_{,j}(\mathbf{x},\mathbf{y})u_j(\mathbf{y}) \right\rfloor dS(\mathbf{y})$$
$$+ \int_S [K_{ij}(\mathbf{x},\mathbf{y})t_j(\mathbf{y}) - H_{ij}(\mathbf{x},\mathbf{y})u_j(\mathbf{y})] dS(\mathbf{y}), \quad \forall \mathbf{x} \in V. \tag{10}$$

Noting Eq. (8) and letting $\mathbf{x}$ tend to S, one obtains the following *traction BIE* (HBIE):

$$c_{ij}(\mathbf{x})t_j(\mathbf{x}) = \int_S \left\lfloor K_{ij}(\mathbf{x},\mathbf{y})t_j(\mathbf{y}) - H_{ij}(\mathbf{x},\mathbf{y})u_j(\mathbf{y}) \right\rfloor dS(\mathbf{y}),$$
$$\forall \mathbf{x} \in S, \tag{11}$$

where $c_{ij} = \frac{1}{2}\delta_{ij}$ assuming S is smooth around $\mathbf{x}$, and

$$K_{ij}(\mathbf{x},\mathbf{y}) = \frac{1}{\pi r}r_{,i}r_{,j}r_{,k}n_k(\mathbf{x}), \tag{12}$$

$$H_{ij}(x,y) = \frac{\mu}{\pi r^2}[(\delta_{ij}r_{,k} + \delta_{jk}r_{,i} - 8r_{,i}r_{,j}r_{,k})r_{,l}n_l$$
$$+ n_i r_{,j}r_{,k} + n_k r_{,i}r_{,j} + \delta_{ik}n_j]n_k(\mathbf{x}) \tag{13}$$

with $n_i(\mathbf{x})$ being the normal at source point $\mathbf{x}$ (Fig. 1). In traction BIE (11), the integral with the K kernel is a CPV integral, while the one with the H kernel is a Hadamard finite-part (HFP) hypersingular integral (see, e.g., Refs. [28–30]). For exterior problems, it has been assumed that the pressure field $p(\mathbf{x})$ vanishes at infinity in the derivation of BIE (11).

CBIE (5) and HBIE (11) with the four kernels U_{ij}, T_{ij}, K_{ij} and H_{ij} can be obtained from those for 2-D elasticity problems by simply setting the Poisson ratio to 0.5 in the corresponding elasticity BIEs.

Some observations on CBIE (5) and HBIE (11) are in order:

(a) For *a Dirichlet problem* where velocity is prescribed on the entire boundary S, CBIE (5) is reduced to

$$\int_S U_{ij}(\mathbf{x},\mathbf{y})t_j(\mathbf{y}) dS(\mathbf{y}) = b_i(\mathbf{x}), \quad \forall \mathbf{x} \in S, \tag{14}$$

where b_i is a known vector from the velocity field; while HBIE (11) is reduced to

$$\frac{1}{2}t_i(\mathbf{x}) = \int_S K_{ij}(\mathbf{x},\mathbf{y})t_j(\mathbf{y}) dS(\mathbf{y}) + d_i(\mathbf{x}), \quad \forall \mathbf{x} \in S, \tag{15}$$

where d_i is another known vector. Eq. (14), a Helmholtz equation of the first kind, is ill-conditioned and not suitable for iterative solvers, while Eq. (15), a Helmholtz equation of the second kind, can yield a system of equations with better conditioning [1,2,21,22].

(b) Any constant pressure field $p(\mathbf{x}) = p_0$, with $u_i = 0$ and $t_i = -p_0 n_i$, is a solution of both Eq. (14) (for *interior* and *exterior* problems) and Eq. (15) (for *interior* problems only). That is, $t_i = -p_0 n_i$ are eigenfunctions of both Eqs. (14) and (15), although corresponding to different eigenvalues, and their solutions for the traction field may not be unique [1,2,21,22].

(c) HBIE has another "defect", that is, an arbitrary constant can be added to the velocity field on a closed contour without changing HBIE (11), due to the fact that

$$\int_{S_k} H_{ij}(x, y)\, \mathrm{d}S(y) = 0,$$

for any closed contour S_k [31]. This means that one has either nonunique solutions of the velocity on the contour if traction is prescribed, or inaccurate evaluation of this contour integral if velocity is given, when HBIE (11) is applied alone. This deficiency with the HBIE and its remedies have been discussed in the context of elasticity in Refs. [32,33].

A remedy to the above-mentioned defects or difficulties is to use CBIE (5) and HBIE (11) together in the form of a linear combination, which has been found to be very effective for 3-D exterior Stokes flow problems in Refs. [24–27], and for both 2-D/3-D interior and exterior potential problems in Refs. [34,35].

In an operator or matrix form, CBIE (5) and HBIE (11) can be written as

$$\tfrac{1}{2}\mathbf{u} + \mathbf{Tu} = \mathbf{Ut} \quad \text{and} \quad -\tfrac{1}{2}\mathbf{t} + \mathbf{Kt} = \mathbf{Hu},$$

respectively. A dual BIE formulation using a linear combination of CBIE (5) and HBIE (11) can be written as

$$\left(\tfrac{1}{2}\mathbf{u} + \mathbf{Tu} - \mathbf{Ut}\right) + \beta\left(-\tfrac{1}{2}\mathbf{t} + \mathbf{Kt} - \mathbf{Hu}\right) = \mathbf{0}, \tag{16}$$

where β is the coupling constant. In this study, a positive β (e.g., $\beta = 1$) has been found to work quite well for all the cases. More discussions on the selections of β can be found in Refs. [34–39] for other cases. Dual BIE formulations have been found to be very effective and efficient for solving acoustic wave, elastic wave, potential and electrostatic problems [34–39]. Dual BIE formulations are especially beneficial to the fast multipole BEM since they provide better conditioning for the BEM systems of equations and thus can facilitate faster convergence when using the iterative solvers.

3. The fast multipole BEM using the dual BIE

The fast multipole algorithms for solving for 2-D potential and elasticity problems have been described in detail in Refs. [18,20]. As a similar case to 2-D elasticity, the 2-D Stokes flow case can be handled using the same algorithms as in 2-D elasticity. The only task is to derive the required expansions, moments and translations. For CBIE (5), the results are extracted from those already available for the 2-D elasticity case given in Ref. [18]. For HBIE (10), the results are derived and provided in this section.

In Ref. [18], it is shown that the two integrals in the CBIE for 2-D elasticity can be represented in complex variables readily if the fundamental solution $U_{ij}(\mathbf{x}, \mathbf{y})$ and $T_{ij}(\mathbf{x}, \mathbf{y})$ are written in complex forms using the results

in 2-D elasticity. By setting the Poisson ratio to 0.5 in these results, we obtain the corresponding expressions for 2-D Stokes flow problems. For example, the first integral in CBIE (5) can be written in the following complex form (cf., Eq. (10) in Ref. [18] for 2-D elasticity):

$$
\begin{aligned}
D_t(z_0) &\equiv [\Delta_1(\mathbf{x}) + \mathrm{i}\Delta_2(\mathbf{x})]_t \\
&\equiv \left\lfloor \int_S U_{1j}(\mathbf{x}, \mathbf{y}) t_j(\mathbf{y})\, \mathrm{d}S(\mathbf{y}) \right\rfloor \\
&\quad + \mathrm{i} \left\lfloor \int_S U_{2j}(\mathbf{x}, \mathbf{y}) t_j(\mathbf{y})\, \mathrm{d}S(\mathbf{y}) \right\rfloor \\
&= \frac{1}{8\pi\mu} \int_S \Big[G(z_0, z)t(z) + \overline{G(z_0, z)}t(z) \\
&\quad - (z_0 - z)\overline{G'(z_0, z)t(z)} \Big]\, \mathrm{d}S(z),
\end{aligned}
\tag{17}
$$

where $\mathrm{i} = \sqrt{-1}$, $\overline{(\ )}$ indicates the complex conjugate, $t = t_1 + \mathrm{i}t_2$ the complex traction, $z_0(= x_1 + \mathrm{i}x_2)$ and $z(= y_1 + \mathrm{i}y_2)$ represent $\mathbf{x}$ and $\mathbf{y}$, respectively, $G(z_0, z) = -\log(z_0 - z)$ the Green's function (in complex form) for 2-D potential problems [5,20], and $G'(z_0, z) \equiv \partial G/\partial z_0$. The integral in Eq. (17) can be used to evaluate readily the U kernel integral in CBIE (5).

Similarly, the complex representation for the second integral with the T kernel in CBIE (5) can be written as follows (cf., Eq. (32) in Ref. [18] for 2-D elasticity):

$$
\begin{aligned}
D_u(z_0) &\equiv [\Delta_1(\mathbf{x}) + \mathrm{i}\Delta_2(\mathbf{x})]_u \equiv \left\lfloor \int_S T_{1j}(\mathbf{x}, \mathbf{y}) u_j(\mathbf{y})\, \mathrm{d}S(\mathbf{y}) \right\rfloor \\
&\quad + \mathrm{i} \left\lfloor \int_S T_{2j}(\mathbf{x}, \mathbf{y}) u_j(\mathbf{y})\, \mathrm{d}S(\mathbf{y}) \right\rfloor \\
&= -\frac{1}{4\pi} \int_S \Big\{ G'(z_0, z)n(z)u(z) \\
&\quad - (z_0 - z)\overline{G''(z_0, z)}\,\overline{n(z)}\,\overline{u(z)} \\
&\quad + \overline{G'(z_0, z)}\big[n(z)\overline{u(z)} + \overline{n(z)}u(z)\big] \Big\}\, \mathrm{d}S(z),
\end{aligned}
\tag{18}
$$

in which $u = u_1 + \mathrm{i}u_2$ and $n = n_1 + \mathrm{i}n_2$ are the complex velocity and normal, respectively.

Applying the relation between the traction and velocity in complex notation, we can show that the first integral with the K kernel in HBIE (11) can be written in the following complex form:

$$
\begin{aligned}
F_t(z_0) &\equiv [F_1(\mathbf{x}) + \mathrm{i}F_2(\mathbf{x})]_t \equiv \left\lfloor \int_S K_{1j}(\mathbf{x}, \mathbf{y}) t_j(\mathbf{y})\, \mathrm{d}S(\mathbf{y}) \right\rfloor \\
&\quad + \mathrm{i} \left\lfloor \int_S K_{2j}(\mathbf{x}, \mathbf{y}) t_j(\mathbf{y})\, \mathrm{d}S(\mathbf{y}) \right\rfloor \\
&= \frac{1}{4\pi} \int_S \Big\{ \big[G'(z_0, z)t(z) + \overline{G'(z_0, z)t(z)} \big] n(z_0) \\
&\quad + \big[\overline{G'(z_0, z)}t(z) - (z_0 - z) \\
&\quad \times \overline{G''(z_0, z)t(z)} \big] \overline{n(z_0)} \Big\}\, \mathrm{d}S(z).
\end{aligned}
\tag{19}
$$

Similarly, the second integral with the H kernel in HBIE (11) can be written as

$$
\begin{aligned}
F_u(z_0) &\equiv [F_1(\mathbf{x}) + iF_2(\mathbf{x})]_u \\
&\equiv \left\lfloor \int_S H_{1j}(\mathbf{x},\mathbf{y})u_j(\mathbf{y})\,dS(\mathbf{y}) \right\rfloor \\
&\quad + i\left\lfloor \int_S H_{2j}(\mathbf{x},\mathbf{y})u_j(\mathbf{y})\,dS(\mathbf{y}) \right\rfloor \\
&= -\frac{\mu}{2\pi}\int_S \Big\{ \big[G''(z_0,z)n(z)u(z) \\
&\quad + \overline{G''(z_0,z)}\,\overline{n(z)}\,\overline{u(z)} \big] n(z_0) \\
&\quad + \big[\overline{G''(z_0,z)}\big(n(z)\overline{u(z)} + \overline{n(z)}u(z) \big) \\
&\quad - (z_0-z)\overline{G'''(z_0,z)\,n(z)\,u(z)} \big] \overline{n(z_0)} \Big\}\,dS(z).
\end{aligned} \tag{20}
$$

It is straightforward to show that expressions (19) and (20) yield the first and second integrals in HBIE (11), respectively, by simply extracting the real and imaginary parts of the right-hand sides of Eqs. (19) and (20).

In the following, we first present the multipole expansions, local expansions and their translations related to Eqs. (17) and (18) in the fast multipole BEM for CBIE (5). Then we discuss the same related to Eqs. (19) and (20) for HBIE (11).

3.1. Multipole expansion (moments) for the U kernel integral

Assuming z_c is a point close to the integration point z (Fig. 2), that is, $|z-z_c| \ll |z_0-z_c|$, we have [18]

$$
G(z_0,z) = \sum_{k=0}^{\infty} O_k(z_0 - z_c)I_k(z - z_c). \tag{21}
$$

where the two auxiliary functions are defined by

$$
I_k(z) = \frac{z^k}{k!}, \quad \text{for} \quad k \geqslant 0, \tag{22}
$$

$$
O_0(z) = -\log(z) \quad \text{and} \quad O_k(z) = \frac{(k-1)!}{z^k}, \quad \text{for} \quad k \geqslant 1. \tag{23}
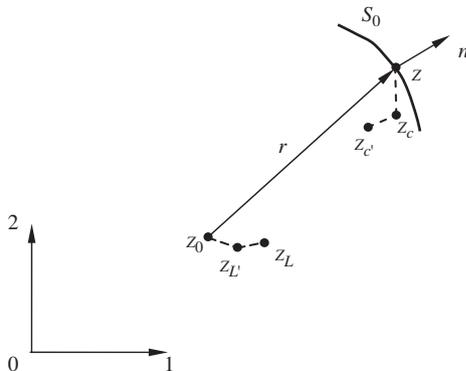$$

Fig. 2. Complex notation and the related points for fast multipole expansions.

Substituting (21) in (17), we obtain the following *multipole expansion* for $D_t(z_0)$ (cf., Eq. (24) in Ref. [18] for 2-D elasticity):

$$
\begin{aligned}
D_t(z_0) = \frac{1}{8\pi\mu}\Bigg[&\sum_{k=0}^{\infty} O_k(z_0 - z_c)M_k(z_c) \\
&+ z_0 \sum_{k=0}^{\infty} \overline{O_{k+1}(z_0 - z_c)M_k(z_c)} \\
&+ \sum_{k=0}^{\infty} \overline{O_k(z_0 - z_c)N_k(z_c)} \Bigg],
\end{aligned} \tag{24}
$$

where the *first set of moments* about z_c are [18]:

$$
M_k(z_c) = \int_{S_0} I_k(z - z_c)t(z)\,dS(z), \quad \text{for} \quad k \geqslant 0 \tag{25}
$$

with S_0 being a subset of S that is far away from the source point, and the *second set of moments* are [18]:

$$
\begin{cases}
N_0 = \int_{S_0} t(z)\,dS(z); \\
N_k(z_c) = \int_{S_0} \big[\overline{I_k(z - z_c)}t(z) - \overline{I_{k-1}(z - z_c)}\,\overline{z}t(z) \big]\,dS(z), \\
\qquad\qquad \text{for} \quad k \geqslant 1.
\end{cases} \tag{26}
$$

3.2. Moment-to-moment (M2M) translation

If point z_c is moved to a new location $z_{c'}$ (Fig. 2), we have [18]

$$
M_k(z_{c'}) = \sum_{l=0}^{k} I_{k-l}(z_c - z_{c'})M_l(z_c), \quad \text{for} \quad k \geqslant 0. \tag{27}
$$

Similarly,

$$
N_k(z_{c'}) = \sum_{l=0}^{k} \overline{I_{k-l}(z_c - z_{c'})}N_l(z_c), \quad \text{for} \quad k \geqslant 0. \tag{28}
$$

These are the *M2M translations* for the moments when z_c is moved to $z_{c'}$. Note that these translation coefficients are symmetrical for the two sets of moments (I_{k-l} and conjugate of I_{k-l}) and coefficients I_{k-l} are exactly the same as used in the 2-D potential case [5,20].

3.3. Local expansion and moment-to-local (M2L) translation

If z_L is a point close to point z_0 (Fig. 2), that is, $|z_0-z_L| \ll |z_c-z_L|$. Expanding $D_t(z_0)$ in (24) about $z_0 = z_L$ using Taylor series expansion, we have the following *local expansion* (cf., Eq. (27) in Ref. [18]):

$$
\begin{aligned}
D_t(z_0) = \frac{1}{8\pi\mu}\Bigg[&\sum_{l=0}^{\infty} L_l(z_L)I_l(z_0 - z_L) \\
&- z_0 \sum_{l=1}^{\infty} \overline{L_l(z_L)I_{l-1}(z_0 - z_L)} \\
&+ \sum_{l=0}^{\infty} K_l(z_L)\overline{I_l(z_0 - z_L)} \Bigg],
\end{aligned} \tag{29}
$$

where the coefficients are given by the following *M2L translations* [18]:

$$L_l(z_L) = (-1)^l \sum_{k=0}^{\infty} O_{l+k}(z_L - z_c)M_k(z_c), \quad \text{for} \quad l \geqslant 0, \quad (30)$$

$$K_l(z_L) = (-1)^l \sum_{k=0}^{\infty} \overline{O_{l+k}(z_L - z_c)}N_k(z_c), \quad \text{for} \quad l \geqslant 0. \quad (31)$$

3.4. Local-to-local (L2L) translation

If the point for the local expansion is moved from z_L to $z_{L'}$ (Fig. 2), the new local expansion coefficients are given by the following *L2L translations* [18]:

$$L_l(z_{L'}) = \sum_{m=l}^{\infty} I_{m-l}(z_{L'} - z_L)L_m(z_L), \quad \text{for} \quad l \geqslant 0, \quad (32)$$

$$K_l(z_{L'}) = \sum_{m=l}^{\infty} \overline{I_{m-l}(z_{L'} - z_L)}K_m(z_L), \quad \text{for} \quad l \geqslant 0. \quad (33)$$

3.5. Expansions for the T kernel integral

Through a similar procedure as used for the U kernel integrals in (17), the multipole expansion of (18) can be written as (cf., Eq. (33) in Ref. [18] for 2-D elasticity):

$$D_u(z_0) = \frac{1}{4\pi} \left[\sum_{k=1}^{\infty} O_k(z_0 - z_c)\tilde{M}_k(z_c) \right.$$
$$+ z_0 \sum_{k=1}^{\infty} \overline{O_{k+1}(z_0 - z_c)}\overline{\tilde{M}_k(z_c)}$$
$$\left. + \sum_{k=1}^{\infty} \overline{O_k(z_0 - z_c)}\tilde{N}_k(z_c) \right], \quad (34)$$

where the two sets of *moments* are:

$$\tilde{M}_k(z_c) = \int_{S_0} I_{k-1}(z - z_c)n(z)u(z)\,\mathrm{d}S(z), \quad \text{for} \quad k \geqslant 1; \quad (35)$$

$$\begin{cases} \tilde{N}_1 = \int_{S_0} \left[n(z)\overline{u(z)} + \overline{n(z)}u(z) \right] \mathrm{d}S(z); \\ \tilde{N}_k(z_c) = \int_{S_0} \left\{ \overline{I_{k-1}(z - z_c)} \left[n(z)\overline{u(z)} + \overline{n(z)}u(z) \right] \right. \\ \left. - \overline{I_{k-2}(z - z_c)}\overline{z}n(z)u(z) \right\} \mathrm{d}S(z), \quad \text{for} \quad k \geqslant 2. \end{cases}$$
$$(36)$$

These moments are similar to those for the U kernel integrals. It can be shown that the M2M, M2L and L2L translations remain the same for the T kernel integrals, except for the fact that $\tilde{M}_0 = \tilde{N}_0 = 0$. In fact, the moments M_k and $\tilde{M}_k$ will be combined, as well as moments N_k and $\tilde{N}_k$, so that only two sets of moments are involved in the M2M and M2L translations. The local expansion for

$D_u(z_0)$ is

$$D_u(z_0) = \frac{1}{4\pi} \left[\sum_{l=0}^{\infty} L_l(z_L)I_l(z_0 - z_L) \right.$$
$$- z_0 \sum_{l=1}^{\infty} \overline{L_l(z_L)I_{l-1}(z_0 - z_L)}$$
$$\left. + \sum_{l=0}^{\infty} K_l(z_L)\overline{I_l(z_0 - z_L)} \right], \quad (37)$$

where the coefficients $L_l(z_L)$ and $K_l(z_L)$ are given by Eqs. (30) and (31) with M_k being replaced by $\tilde{M}_k$, and N_k by $\tilde{N}_k$, respectively.

3.6. Expansions for the HBIE

To derive the multipole expansions and local expansions for HBIE (11), specifically, for its two integrals in complex forms (19) and (20), one can simply take the derivatives of the local expansions for the two integrals in CBIE, that is, Eqs. (29) and (37), respectively, and then invoke the constitutive relation, that is, Eq. (4) written in the complex form. The result of the local expansion for the first integral $F_t(z_0)$ in (19) for the HBIE is

$$F_t(z_0) = \frac{1}{4\pi} \left\{ \left[\sum_{l=0}^{\infty} L_{l+1}(z_L)I_l(z_0 - z_L) \right. \right.$$
$$\left. + \sum_{l=0}^{\infty} \overline{L_{l+1}(z_L)I_l(z_0 - z_L)} \right] n(z_0)$$
$$+ \left[-z_0 \sum_{l=1}^{\infty} \overline{L_{l+1}(z_L)I_{l-1}(z_0 - z_L)} \right.$$
$$\left. \left. + \sum_{l=0}^{\infty} K_{l+1}(z_L)\overline{I_l(z_0 - z_L)} \right] \overline{n(z_0)} \right\}, \quad (38)$$

in which, the expansion coefficients $L_l(z_L)$ and $K_l(z_L)$ are given by the same M2L translations in (30) and (31), respectively. That is, the same sets of moments M_k and N_k used for $D_t(z_0)$ are used for $F_t(z_0)$ directly.

Similarly, it can be shown that the local expansion for the second integral $F_u(z_0)$ in (20) for the HBIE is

$$F_u(z_0) = \frac{\mu}{2\pi} \left\{ \left[\sum_{l=0}^{\infty} L_{l+1}(z_L)I_l(z_0 - z_L) \right. \right.$$
$$\left. + \sum_{l=0}^{\infty} \overline{L_{l+1}(z_L)I_l(z_0 - z_L)} \right] n(z_0)$$
$$+ \left[-z_0 \sum_{l=1}^{\infty} \overline{L_{l+1}(z_L)I_{l-1}(z_0 - z_L)} \right.$$
$$\left. \left. + \sum_{l=0}^{\infty} K_{l+1}(z_L)\overline{I_l(z_0 - z_L)} \right] \overline{n(z_0)} \right\}, \quad (39)$$

in which $L_l(z_L)$ and $K_l(z_L)$ are given by Eqs. (30) and (31) with M_k being replaced by $\tilde{M}_k$, and N_k by $\tilde{N}_k$, respectively. Again, the same sets of moments $\tilde{M}_k$ and $\tilde{N}_k$ used for

$D_u(z_0)$ are used for $F_u(z_0)$, and all the M2M, M2L and L2L translations for the HBIE remain the same as used for the CBIE.

The details of the fast multipole algorithms for solving 2-D Stokes problems are similar to the ones for 2-D potential and elasticity problems, which have been described in details in Refs. [18,20]. Pre-conditioners for the fast multipole BEM are crucial for its convergence and computing efficiency. In this study, the block diagonal preconditioner is employed, which is formed on each leaf using direct evaluations of the kernels on the elements within that leaf. When the problem size is large, the estimated cost of the entire process is $O(N)$ with N being the number of equations, if the number of terms in the multipole expansions and the number of elements in a leaf are kept constant (see Ref. [19] for an estimate).

In this study, we employ constant boundary elements (straight line segment with one node) to discretize the BIEs. All the moments are evaluated analytically, as well as the integrations of the kernels in the near-field direct evaluations.

4. Numerical examples

We present three numerical examples to demonstrate the accuracy and efficiency of the new fast multipole BEM for 2-D Stokes flow problems using the dual BIE formulation. All the computations are done on a Pentium IV laptop PC with a 2.4 GHz CPU and 1 GB RAM. In all the examples, the number of terms for both multipole and local expansions are set to 20, the maximum number of elements in a leaf to 100, and the coupling constant $\beta = 1$ for the dual BIE (CHBIE) formulation.

4.1. Flow due to the rotation of a circular cylinder

The flow in an infinite 2-D medium due to a rotating circular cylinder is considered first (Fig. 3). The radius of the cylinder is a and the angular velocity is Ω. Solution of this problem exists [40], that is, in the polar coordinate system, we have

$$u_r(r,\theta) = 0, \quad u_\theta(r,\theta) = \Omega a^2/r \quad \text{and} \quad \sigma_{r\theta}(r,\theta) = -2\mu\Omega a^3/r^2 \tag{40}$$

which can be used to verify the BEM solutions. The velocity is specified on the boundary using the above results and the tractions are sought using the BEM. For the fast multipole BEM solutions, the tolerance for convergence is set to 10^{-6}.

Table 1 shows the results of the tractions at the boundary computed by the fast multipole BEM using both the CBIE and CHBIE formulations (HBIE cannot provide solutions in this case due to defect (c) mentioned in Section 2). Although both BIE formulations give results of comparable accuracies, the CHBIE converges much faster than the CBIE, as indicated by the number of
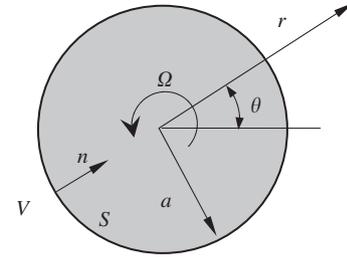

Fig. 3. A rotating cylinder in an infinite fluid.

Table 1
Traction t_y at $(a, 0)$ and numbers of iterations used in fast multipole BEM

DOFs	t_y ($\times \mu\Omega a$)		Number of iterations	
	CBIE	CHBIE	CBIE	CHBIE
80	1.9999	1.9891	16	7
160	2.0003	1.9936	18	7
320	2.0054	1.9965	13	7
640	2.0028	1.9981	13	4
1280	2.0011	1.9990	14	4
2560	2.0005	1.9995	16	4
5120	1.9997	1.9998	21	4
10,240	1.9997	1.9999	28	4
20,480	2.0007	1.9999	32	4
Exact solution	2.0000			

iterations used, which are also listed in Table 1. Fig. 4 is a plot of the traction components on the boundary of the cylinder with 40 elements and using CHBIE. Fig. 5 shows the velocity computed at points inside the fluid domain using Eq. (5) with the same mesh and the CHBIE. Both results demonstrate that the fast multipole BEM results are quite accurate with only 40 constant elements.

The CPU times used for the fast multipole BEM based on the CBIE and CHBIE approaches are plotted in Fig. 6, which shows significant advantage of the CHBIE formulation than the CBIE formulation. For example, for the model with 10,240 elements (DOFs = 20,480), the fast multipole BEM with CHBIE used about 17 s of CPU time, while the BEM with the CBIE used about 92 s, which is about four times slower. High condition numbers are observed for the CBIE and very low condition numbers for the CHBIE with a direct solver, which is consistent with the solution efficiency with the iterative solver.

4.2. Shear flow between two parallel plates

The flow between two parallel plates (Fig. 7) is studied next using the CBIE, HBIE and CHBIE formulations. The top plate is moving with a constant speed v_0 in the x-direction and no slip condition is assumed between the plates and fluid. The analytical solution for this problem is

$$u_x(x,y) = v_0 y/h, \quad u_y = 0 \quad \text{and} \quad \sigma_x = \sigma_y = 0, \quad \sigma_{xy} = \mu v_0/h. \tag{41}$$
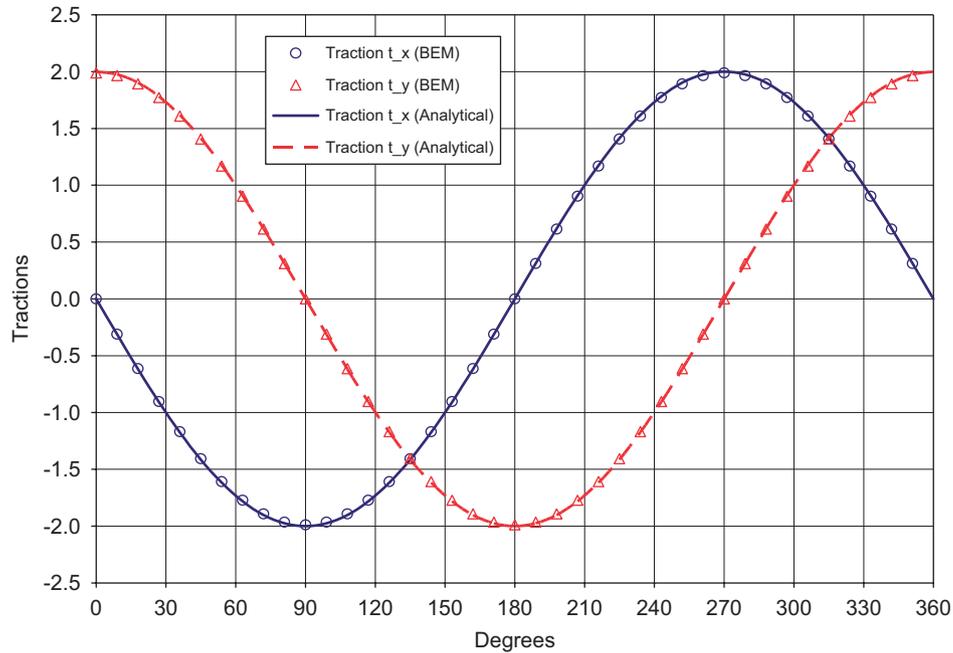
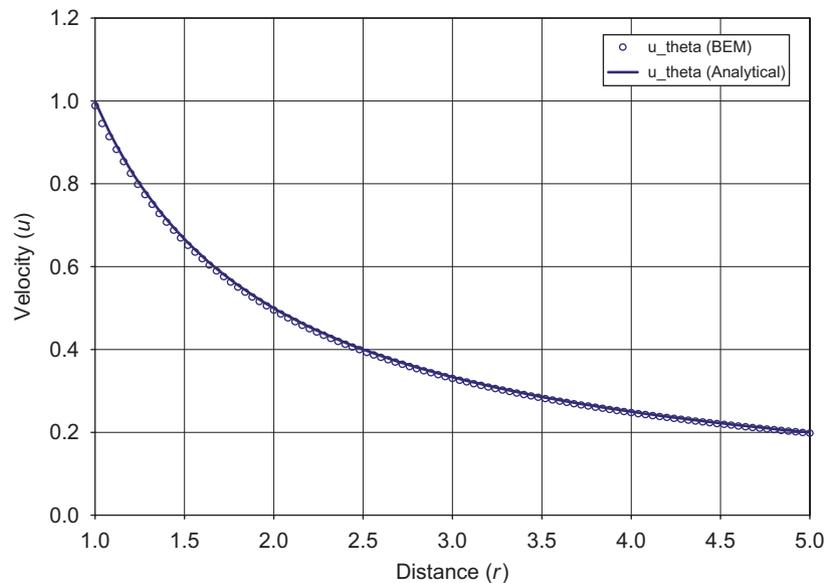Fig. 4. Computed tractions on boundary S (with 40 elements).

Fig. 5. Velocity u_θ computed at points inside the fluid domain V (with 40 elements).

The purpose of this study is to investigate the behaviors of the BEM solutions as the ratio h/L approaches zero, that is, when the fluid domain becomes a narrow channel. The narrow spaces between two fingers of an MEMS comb-drive device closely resemble the configuration studied in this example with small ratios of h/L.

Mixed boundary conditions are used in this example so that all three BIE formulations, that is, CBIE (5), HBIE (11) and the CHBIE (16), can be tested. For the lower boundary, zero velocities are specified, while for the upper boundary, velocities are given as $u_x = v_0$ and $u_y = 0$. For

the two vertical boundaries, tractions are given as $t_x = 0$, $t_y = \mu v_0/h$ at $x = L$; and $t_x = 0$, $t_y = -\mu v_0/h$ at $x = 0$. The tolerance for convergence in the fast multipole BEM is also set to 10^{-6} in this case.

Table 2 shows the dimensions, BEM discretizations, computed tractions at the mid-point of the lower boundary, and numbers of iterations used in the fast multipole BEM solutions with the three BIE formulations. It is observed that as the ratio of h/L becomes smaller, more iterations are needed for the CBIE formulation, while about the same numbers of iterations are needed for the
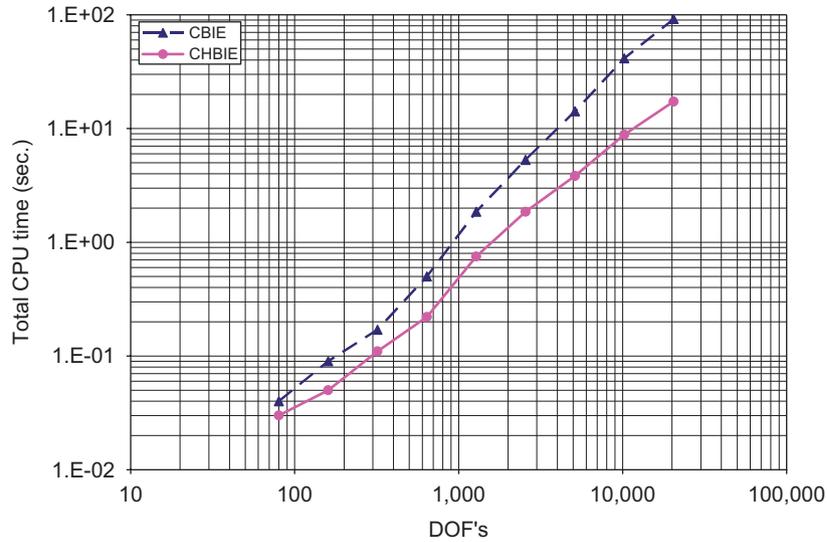
Fig. 6. Total CPU time used for solving the rotating cylinder problem by the fast multipole BEM with CBIE and CHBIE (log–log scale).
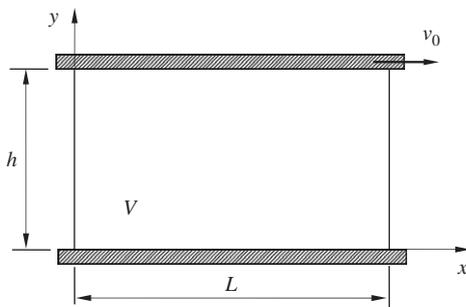

Fig. 7. Shear flow between two parallel plates.

HBIE and CHBIE formulations. These results indicate the poor conditioning of the CBIE formulation, while good and improved conditionings of the HBIE and CHBIE formulations, respectively. Most interesting is the fact that even at $h/L = 10^{-6}$, all three BIE formulations can still provide reasonably good results of the tractions. The results by the HBIE and CHBIE are slightly less accurate than those by the CBIE at small h/L, which may be caused by the extremely small elements on the two small vertical edges. Recall that for 2-D problems, the finite-part of the hypersingular integral is proportional to $1/R$ with R being the element length here. If R is very small, as is tested in this case, $1/R$ can be very large and cause numerical errors in the BEM systems of equations. In fact, the BEM code fails when the ratio h/L is smaller than 10^{-6} for this example, due to the existence of the hypersingular kernel H. This is different from the results reported in Ref. [34] for electrostatic MEMS problems, where the ratio h/L of a beam can reach 10^{-16} for the dual BIE formulation that does not have the hypersingular kernel.

This example demonstrates that the dual BIE formulation can facilitate fast convergence for the fast multipole BEM even when the domain of consideration is extremely

thin. This is consistent with the conclusions with the dual BIE approach for fast multipole BEM in the context of electrostatic analysis of MEMS models [34,35].

4.3. Flow through a channel with many cylinders

We next tackle interior Dirichlet problem, that is, Stokes flows through a channel placed with one or multiple cylinders. The dimensions of the channel are shown in Fig. 8. At the inlet of the channel ($x = 0$), the flow has a parabolic velocity profile:

$$u_x(0, y) = 4v_0(1 - y/h)y/h \text{ and } u_y(0, y) = 0, \tag{42}$$

where v_0 is the maximum value of the velocity. At the outlet of the channel ($x = L$), the same velocity profile is assumed (Fig. 8), that is, the flow is assumed to have recovered from the disturbances by the cylinder(s) placed in the middle section of the channel. On the upper and lower boundaries and all cylinder boundaries, no slip boundary conditions are assumed. For this test, the tolerance for convergence for the GMRES solver is set to 10^{-5}.

First, the case with one circular cylinder placed in the center of the channel is studied, with $L = 2h$ and $a = 0.1h$. Fig. 9 shows the velocity vector plot within the fluid obtained by using the CHBIE. There are about 800 points distributed evenly inside the domain where the velocity is evaluated using integral representation in Eq. (5) after the tractions are obtained from the BEM solutions. Table 3 shows the total fluid force applied on the cylinder and evaluated by integrating the obtained traction field on the boundary of the cylinder (assuming a unit depth). There are 600 elements on the outer boundary and the number of elements on the cylinder increases. Both CBIE and CHBIE are used and the results for the total force on the cylinder are very stable with the CBIE, while those with the CHBIE increase slowly to reach a stable value. The errors with the

Table 2
Comparison of the three BIE formulations for the shear flow problem

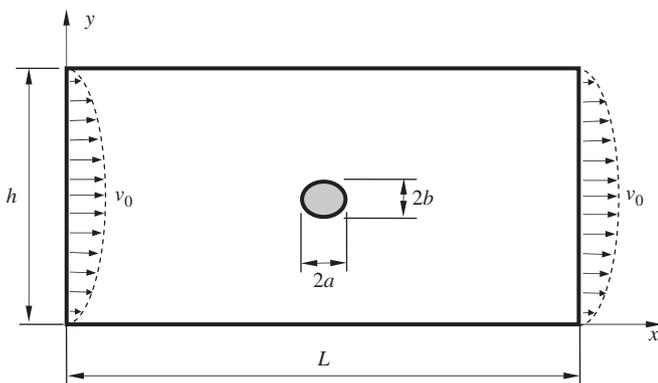| h/L	Number of elements on edges L and h	Traction t_x ($\times \mu v_0/h$) at $(L/2, 0)$			Number of iterations		
		CBIE	HBIE	CHBIE	CBIE	HBIE	CHBIE
1.0E+00	100/100	−0.99980	−1.00135	−0.99961	15	17	16
1.0E−01	100/20	−0.99998	−1.00264	−1.00185	25	21	21
1.0E−02	100/10	−1.00000	−1.00027	−1.00021	73	68	69
1.0E−03	100/5	−1.00000	−0.99985	−0.99988	142	67	67
1.0E−04	100/3	−1.00000	−0.99931	−0.99935	185	65	94
1.0E−05	100/2	−0.99998	−0.99943	−0.99514	227	49	70
1.0E−06	100/1	−0.99979	−0.99322	−0.98546	298	40	54
Exact solution		−1.00000					

Fig. 8. Channel flow around a cylinder.

CHBIE may be due to the finite-part integrals in the HBIE on curved boundaries computed with constant elements which can introduce numerical errors (see also Ref. [35] for 3-D potential case). It is also observed that the condition numbers of the CBIE and CHBIE equations for this interior problem are high, although the fast multipole BEM can solve the problem using both BIEs. As shown in Table 3, the number of iterations with the CBIE increases as the model size increases, while numbers of iterations with the CHBIE are almost constant and only about one half to one quarter of those for the CBIE.

Next, the models with multiple elliptic cylinders placed in the middle section of a channel with $L = 3h$ are studied. These models are motivated by the examples presented by Greengard et al. in Ref. [7], with different geometries, boundary conditions and numbers of elements. Fig. 10(a) shows the velocity plot for a 5×5 array of elliptic cylinders with a uniform distribution, while Fig. 10(b) shows the velocity field with a random distribution, both using CHBIE with 16,600 DOFs. For the uniform distribution, 59 iterations are used (381 s CPU time), while for the random distribution, 82 iterations are used (491 s CPU time). It is observed that when more cylinders are placed in the same space or when cylinders are distributed randomly, the iteration numbers for the BEM solutions will increase, due to the intensified interactions between the cylinders as

discussed in Ref. [22]. Fig. 10(c) shows a larger model with 13×13 elliptic cylinders packed evenly in the middle section of the channel. The model has 103,000 DOFs and both CBIE and CHBIE are applied. The numbers of iterations increase dramatically for this large model. CBIE used 248 iterations (9130 s CPU time), while CHBIE used 168 iterations (6631 s CPU time). Again, the advantage of the CHBIE formulation with the fast multipole BEM is evident.

5. Discussions

A new fast multipole BEM for solving large-scale 2-D Stokes flow problems is presented in this paper based on a dual direct BIE formulation. The dual BIE approach, using a linear combination of the CBIE and HBIE, can significantly improve the conditioning of the BEM systems of equations and thus can facilitate faster convergence when the fast multipole BEM is applied. The dual BIE also provides better conditioning for analyzing problems with narrow domains or thin features. The fast multipole formulations are presented for both CBIE and HBIE for the 2-D Stokes flow problems. These fast multipole formulations are based on the complex variable approach that yields very compact results. For the HBIE, local expansions can be obtained by directly taking derivatives of the local expansions for the CBIE using the complex notation. Thus the same moments and all M2M, M2L and L2L translations as used for the CBIE can be applied for the HBIE. Three numerical examples are presented that clearly demonstrate the accuracy and efficiency of the developed fast multipole BEM with the dual BIE formulation for solving large-scale 2-D Stokes flow problems.

The due BIE formulation proposed in this paper may be improved by the techniques used in Refs. [1,2,21,22] to form complete indirect BIE formulations in order to obtain equations with better conditioning. The fast multipole BEM developed in this paper can also be applied readily to other indirect BIE formulations [21,22]. To improve the accuracy and efficiency of the fast multipole BEM for solving large-scale models, constant elements can be
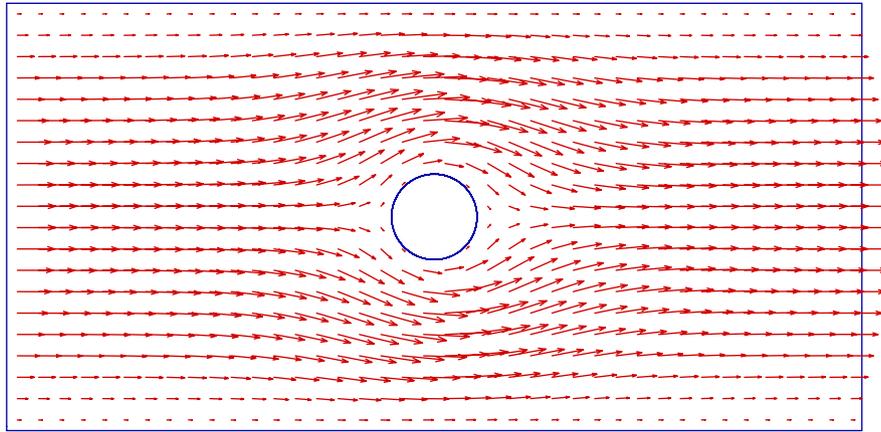
Fig. 9. Vector plot of the velocity field for one circular cylinder with $a = 0.1h$ and $L = 2h$.

Table 3
Computed force F on the cylinder with CBIE and CHBIE

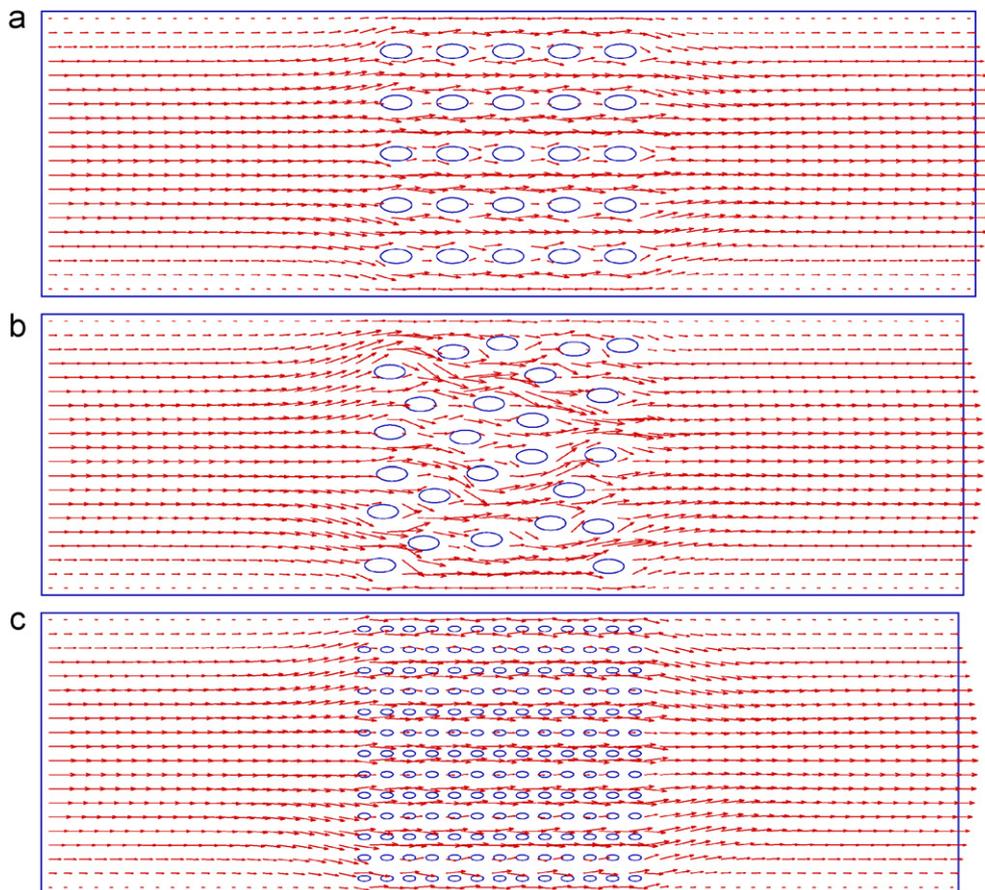| Number of elements on cylinder	Total DOFs	Force F ($\times \mu v_0$)		No. of iterations		CPU time (s)	
		CBIE	CHBIE	CBIE	CHBIE	CBIE	CHBIE
320	1840	16.21	15.38	23	12	9.8	5.7
640	2480	16.21	15.76	26	12	16.2	8.5
1280	3760	16.21	15.96	28	9	30.8	12.0
2560	6320	16.21	16.06	28	9	68.8	26.2
5120	11,440	16.21	16.11	33	9	137.8	45.2
10,240	21,680	16.21	16.14	37	9	277.1	82.1

Fig. 10. Various BEM models of the channel with many elliptic cylinders ($L = 3h$).

replaced with higher-order elements (such as linear and quadratic elements). This will be especially beneficial to the HBIE since the finite-part integrals can be evaluated more accurately on curved boundaries with higher-order elements than with the constant elements as used in this study. Parallel computing with the fast multipole BEM [21,22,41] can also be employed to further improve the computational efficiencies. Field evaluations inside the domain, for which direct evaluation is used in this study, can be performed with the fast multipole BEM as well [10].

The developed dual BIE approach together with the efficient fast multipole BEM can be extended to study other 2-D as well as 3-D Stokes flow problems, such as calculating the damping forces in MEMS [24–27,42], problems with slip boundary conditions or Stokes flows interacting with deformable bodies [40,43,44]. Quasi-dynamic analysis of particles in Stokes flows is also possible using the developed fast multipole solver for fast evaluation of the solution in each time step [22]. Combining the Stokes fast multipole BEM code with the one for elasticity problems to study coupled fluid–structure interaction problems is also possible and will be an interesting research topic for applications in analyzing MEMS devices and biological systems.

Acknowledgments

References

[1] Pozrikidis C. Boundary integral and singularity methods for linearized viscous flow. New York: Cambridge University Press; 1992.

[2] Power H, Wrobel LC. Boundary integral methods in fluid mechanics. Southampton: Computational Mechanics Publications; 1995.

[3] Rokhlin V. Rapid solution of integral equations of classical potential theory. J Comp Phys 1985;60:187–207.

[4] Greengard LF, Rokhlin V. A fast algorithm for particle simulations. J Comput Phys 1987;73(2):325–48.

[5] Greengard LF. The rapid evaluation of potential fields in particle systems. Cambridge: The MIT Press; 1988.

[6] Peirce AP, Napier JAL. A spectral multipole method for efficient solution of large-scale boundary element models in elastostatics. Int J Numer Methods Eng 1995;38:4009–34.

[7] Greengard LF, Kropinski MC, Mayo A. Integral equation methods for Stokes flow and isotropic elasticity in the plane. J Comput Phys 1996;125:403–14.

[8] Greengard LF, Helsing J. On the numerical evaluation of elastostatic fields in locally isotropic two-dimensional composites. J Mech Phys Solids 1998;46(8):1441–62.

[9] Fu Y, Klimkowski KJ, Rodin GJ, Berger E, Browne JC, Singer JK, et al. A fast solution method for three-dimensional many-particle problems of linear elasticity. Int J Numer Methods Eng 1998;42: 1215–29.

[10] Yoshida K, Nishimura N, Kobayashi S. Application of fast multipole Galerkin boundary integral equation method to crack problems in 3D. Int J Numer Methods Eng 2001;50:525–47.

[11] Yoshida K, Nishimura N, Kobayashi S. Application of new fast multipole boundary integral equation method to elastostatic crack problems in three dimensions. J Struct Eng 2001;47A(March): 169–79.

[12] Richardson JD, Gray LJ, Kaplan T, Napier JA. Regularized spectral multipole BEM for plane elasticity. Eng Anal Bound Elem 2001;25: 297–311.

[13] Popov V, Power H. An O(N) Taylor series multipole boundary element method for three-dimensional elasticity problems. Eng Anal Boundary Elem 2001;25(1):7–18.

[14] Popov V, Power H, Walker SP. Numerical comparison between two possible multipole alternatives for the BEM solution of 3D elasticity problems based upon Taylor series expansions. Eng Anal Boundary Elem 2003;27(5):521–31.

[15] Lai Y-S, Rodin GJ. Fast boundary element method for three-dimensional solids containing many cracks. Eng Anal Boundary Elem 2003;27(8):845–52.

[16] Masters N, Ye W. Fast BEM solution for coupled 3D electrostatic and linear elastic problems. Eng Anal Boundary Elem 2004;28(9): 1175–86.

[17] Yao Z, Kong F, Wang H, Wang P. 2D simulation of composite materials using BEM. Eng Anal Boundary Elem 2004;28(8):927–35.

[18] Liu YJ. A new fast multipole boundary element method for solving large-scale two-dimensional elastostatic problems. Int J Numer Methods Eng 2005;65(6):863–81.

[19] Nishimura N. Fast multipole accelerated boundary integral equation methods. Appl Mech Rev 2002;55(4 (July)):299–324.

[20] Liu YJ, Nishimura N. The fast multipole boundary element method for potential problems: a tutorial. Eng Anal Boundary Elem 2006; 30(5):371–81.

[21] Gomez JE, Power H. A multipole direct and indirect BEM for 2D cavity flow at low Reynolds number. Eng Anal Boundary Elem 1997; 19:17–31.

[22] Mammoli AA, Ingber MS. Stokes flow around cylinders in a bounded two-dimensional domain using multipole-accelerated boundary element methods. Int J Numer Methods Eng 1999;44: 897–917.

[23] Ding J, Ye W. A fast integral approach for drag force calculation due to oscillatory slip stokes flows. Int J Numer Methods Eng 2004; 60(9):1535–67.

[24] Frangi A. A fast multipole implementation of the qualocation mixed-velocity-traction approach for exterior Stokes flows. Eng Anal Boundary Elem 2005;29(11):1039–46.

[25] Frangi A, Gioia Ad. Multipole BEM for the evaluation of damping forces on MEMS. Comput Mech 2005;37(1):24–31.

[26] Frangi A, Tausch J. A qualocation enhanced approach for Stokes flow problems with rigid-body boundary conditions. Eng Anal Boundary Elem 2005;29(9):886.

[27] Frangi A, Spinola G, Vigna B. On the evaluation of damping in MEMS in the slip–flow regime. Int J Numer Methods Eng 2006;68: 1031–51.

[28] Krishnasamy G, Rizzo FJ, Rudolphi TJ. Hypersingular boundary integral equations: their occurrence, interpretation, regularization and computation. In: Banerjee PK, et al., editors. Developments in boundary element methods. London: Elsevier Applied Science Publishers; 1991 [Chapter 7].

[29] Mukherjee S. CPV and HFP integrals and their applications in the boundary element method. Int J Solids Struct 2000;37(45): 6623–34.

[30] Mukherjee S. Finite parts of singular and hypersingular integrals with irregular boundary source points. Eng Anal Boundary Elem 2000;24: 767–76.

[31] Liu YJ, Rudolphi TJ. Some identities for fundamental solutions and their applications to weakly-singular boundary element formulations. Eng Anal Boundary Elem 1991;8(6):301–11.

[32] Frangi A, Novati G. Symmetric BE method in two-dimensional elasticity: evaluation of double integrals for curved elements. Comput Mech 1996;19:58–68.

[33] Perez-Gavilan JJ, Aliabadi MH. Symmetric Galerkin BEM for multi-connected bodies. Commun Numer Methods Eng 2001;17:761–70.

[34] Liu YJ. Dual BIE approaches for modeling electrostatic MEMS problems with thin beams and accelerated by the fast multipole method. Eng Anal Boundary Elem 2006;30(11):940–8.

[35] Liu YJ, Shen L. A dual BIE approach for large-scale modeling of 3-D electrostatic problems with the fast multipole boundary element method. Int J Numer Methods Eng 2007;71:837–55.

[36] Liu YJ, Rizzo FJ. A weakly-singular form of the hypersingular boundary integral equation applied to 3-D acoustic wave problems. Comput Methods Appl Mech Eng 1992;96:271–87.

[37] Liu YJ, Rizzo FJ. Hypersingular boundary integral equations for radiation and scattering of elastic waves in three dimensions. Comput Methods Appl Mech Eng 1993;107:131–44.

[38] Liu YJ, Rizzo FJ. Scattering of elastic waves from thin shapes in three dimensions using the composite boundary integral equation formulation. J Acoust Soc Am 1997;102(2 (Part 1, August)): 926–32.

[39] Shen L, Liu YJ. An adaptive fast multipole boundary element method for three-dimensional acoustic wave problems based on the Burton–Miller formulation. Comput Mech 2007;40(3):461–72.

[40] Pozrikidis C. Fluid dynamics—theory, computation and numerical simulation. Boston: Kluwer Academic Publishers; 2001.

[41] Gomez JE, Power H. A parallel multipolar indirect boundary element method for the Neumann interior Stokes flow problem. Int J Numer Methods Eng 2000;48(4):523–43.

[42] Mukherjee S, Telukunta S, Mukherjee YX. BEM modeling of damping forces on MEMS with thin plates. Eng Anal Boundary Elem 2005;29:1000–7.

[43] Power H. The interaction of a deformable bubble with a rigid wall at small Reynolds number: a general approach via integral equations. Eng Anal Boundary Elem 1997;19(4):291.

[44] Zhu G, Mammoli AA, Power H. A 3-D indirect boundary element method for bounded creeping flow of drops. Eng Anal Boundary Elem 2006;30(10):856.